

Continuous sheath-less microfluidic separation of nonmagnetic microparticles in a novel viscoelastic-based ferrofluid

Jun Zhang^a, Sheng Yan^b, Dan Yuan^b, Qianbin Zhao^b, Say Hwa Tan^c, Nam-Trung Nguyen^{c*}, Weihua Li^{b*}

^a School of Mechanical Engineering, Nanjing University of Science and Technology, Nanjing 210094, China

^b School of Mechanical, Materials and Mechatronic Engineering, University of Wollongong, Wollongong, NSW 2522, Australia, Fax: +61 2 4221 3238; Tel: +61 2 4221 3490; E-mail: weihuali@uow.edu.au

^c Queensland Micro and Nanotechnology Centre, Griffith University, Brisbane QLD 4111, Australia, Fax: +61 07 373 58021; Tel: +61 (07) 373 53921; E-mail: nam-trung.nguyen@griffith.edu.au

Abstract:

Separation of microparticles has a broad of applications in biomedicine, industry and clinical diagnosis. In a conventional aqueous ferrofluid, separation of microparticles usually employs a sheath flow or two offset magnets to confine particle streams for downstream particle sorting, which complicates the fluid control and device fabrication, and dilutes particle sample. In this work, we propose and develop a novel viscoelastic-based ferrofluid by replacing the Newtonian base medium of the conventional ferrofluid with non-Newtonian poly(ethylene oxide) (PEO) aqueous solution. The properties of both viscoelastic 3D focusing and negative magnetophoresis of the viscoelastic-based ferrofluid were verified and investigated. In addition, by employing the both properties in a series-connected manner, continuous and sheathless separation of non-magnetic particles based on particle size has been demonstrated. The novel viscoelastic ferrofluid is expected to bring more flexibility and versatility to the design and functionality in microfluidic devices.

Introduction

Manipulation of micro-particles in a microfluidic platform is an indispensable tool for biomedical applications. For example, focusing and ordering micro-particles along a specific single path in three dimensional (3D) enables single-cell level detection and analysis in on-chip flow cytometry. Focusing randomly distributed particles into one or several positions can be employed to enrich [1] or filtrate [2] bio-particles. Separation of target bio-particles from massive background bio-particles according to the unique biophysical properties is a routine process in medical laboratories for down-stream biochemical analysis, disease diagnosis and therapeutics [3].

Many techniques have been developed to manipulate microparticles in microfluidics. According to the source of the manipulating forces, they are categorised as active and passive techniques. Active techniques rely on external electric [4], magnetic [5, 6], acoustic [7] or optical [8] force fields, whereas passive techniques depend entirely on the channel geometry and intrinsic hydrodynamic forces, such as pinched flow fractionation [9], deterministic lateral displacement [10], hydrophoresis [11], inertial microfluidics [12] and viscoelastic focusing [13].

Magnetophoresis was first proposed to describe the behaviour of a magnetic particle moving through a viscous medium under the influence of an external magnetic field [14]. The functionalized magnetic beads were used to label bioparticles because most of bioparticles in nature are non-magnetic [15]. However, the label-based methods are labour-intensive and time-consuming, and magnetic moments of beads may vary significantly [16]. Later, a label-free technique that uses negative magnetophoresis to manipulate and separate non-magnetic bioparticles was proposed by suspending them in a magnetic fluid, such as paramagnetic salts [17] or ferrofluid [18]. In negative magnetophoresis, effective magnetic dipole moments are induced within the microparticles, and they experience a magnetic buoyancy force along the weaker field direction under non-uniform magnetic fields [16]. Paramagnetic solutions such as MnCl_2 and GdCl_3 have a poor magnetic susceptibility. In order to induce sufficient magnetophoresis of particles, salt concentration must be very high which may destruct its biocompatibility [19]. Alternatively, strong magnets need to be brought very close to the nonmagnetic particles.

Ferrofluids are opaque colloidal suspension of magnetic nanoparticles (made of magnetite, Fe_3O_4 , and usually of 10 nm in diameter) in pure water or organic oil with surfactants coated to prevent cohesion [20]. Synthesis of biocompatible ferrofluids has been reported using appropriate stabilizing surfactants [5, 18]. Because ferrofluids usually have a much higher magnetic susceptibility than that of paramagnetic solutions, permanent magnets or electromagnets are sufficient to induce enough magnetophoretic force to manipulate non-magnetic particles in microfluidics [21]. Many previous works have reported focusing and separation of microparticles and cells using ferrofluid in microfluidics [5, 16, 18, 22-24]. In most works, the non-magnetic particle suspension needs to be first confined by a co-flowing sheath flow, and in the downstream an external magnetic field acts on the nonmagnetic particles and deflects them into different paths [16, 24]. However, the utilization of sheath flow not only complicates the flow control and device fabrication, but also dilutes the sorted particles [23]. Alternatively, the employment of two offset magnets or two arrays of

permanent magnets in a straight microchannel have been proposed to achieve sheath-free focusing and continuous separation of particles [25]. The main challenge of using two offset magnets lies in positioning two magnets precisely in the microfluidic device because there is a strong magnetic attractive or repulsive force between two magnets. Furthermore, determining the exact distances between two offset magnets and microchannel is laborious.

In conventional ferrofluids, the base medium is Newtonian fluid. Recently, the elastic property of non-Newtonian fluid has been extensively studied to manipulate micro-particles in microfluidics [26, 27]. So far, the proposed viscoelastic mediums for particle viscoelastic focusing include solutions of poly(ethylene oxide) (PEO) [28-31], polyvinylpyrrolidone (PVP) [3, 32], DNA [33], polyacrylamide (PAM) [34] and hyaluronic acid (HA) [35]. The elastic force induced by the normal stress difference in these viscoelastic fluids will focus particles into the zero shear rate regions (channel centerline or corners in a square channel) [33, 36]. Under a proper flow rate, the multiple equilibrium positions can be further reduced to one at the centreline due to the synergetic effects of inertial and viscoelasticity [37].

In this work, we will explore the possibilities of combining these two properties (negative magnetophoresis and viscoelastic focusing) together in a single medium, by suspending magnetic nanoparticles in a viscoelastic base medium. The individual properties of negative magnetophoretic and viscoelastic focusing will be verified and investigated. Then, through combining both properties in the design of microfluidic devices, sheath-less size-dependent separation of non-magnetic microparticles will be demonstrated through viscoelastic pre-focusing and magnetophoretic deflection in a serial manner. Empowering both superior properties in a single ferrofluid will bring more flexibility and versatility for the design and implementation of particle focusing and separation in microfluidics.

2. Mechanism

2.1 Negative magnetophoretic force

When non-magnetic particles suspended in a ferrofluid are exposed to a non-uniform magnetic field, the negative magnetophoretic force on the non-magnetic particles can be expressed as [15, 17]:

$$\mathbf{F}_m = 3\mu_0 V_p \frac{\chi_p - \chi_f}{3 + \chi_p + \chi_f} (\mathbf{H} \cdot \nabla) \mathbf{H} \quad (1)$$

where $\mu_0 = 4\pi \times 10^{-7}$ H/m is the permeability of free space, V_p is the volume of the particle, χ_p is the magnetic susceptibility of the particle, χ_f is the magnetic susceptibility of the ferrofluid, and \mathbf{H} is the magnetic field at the centre of particle. Because the magnetic susceptibility of

non-magnetic particle is smaller than that of ferrofluid, $\chi_p < \chi_f$, the negative magnetophoretic force \mathbf{F}_m directs along the inverse direction of magnetic field gradient. When χ_p and χ_f are at least three orders of magnitude smaller than 1 for the nonmagnetic particles and the diluted ferrofluid, equation (1) can be further simplified as [6]:

$$\mathbf{F}_m = \mu_0 V_p (\chi_p - \chi_f) (\mathbf{H} \cdot \nabla) \mathbf{H} \quad (2)$$

2.2 Elastic force

Particles immersed in a viscoelastic fluid experience an elastic force due to the intrinsic properties of the suspending medium. The elastic effects of a viscoelastic fluid in channel flow can be characterised by the Weissenberg number W_i [37]:

$$W_i = \frac{\lambda}{t_f} = \lambda \dot{\gamma} \quad (3)$$

where λ , t_f and $\dot{\gamma}$ are the relaxation time of the viscoelastic fluid, the characteristic time of the channel flow and the average fluid shear rate, respectively. The characteristic time is approximately equal to the inverse of the characteristic shear rate $\dot{\gamma}$, which can be expressed as $2U/w$ or $2\lambda Q/hw^2$ in a rectangular channel, here U is the average fluid velocity, Q is the flow rate, w and h are the width and height of the channel, respectively [37]. In a viscoelastic fluid, both the first and second normal stresses, $N_1 = \tau_{xx} - \tau_{yy}$ and $N_2 = \tau_{yy} - \tau_{zz}$ contribute to particle lateral migration, here τ is the normal stress caused by the velocity gradient and the vorticity in the flow. Because N_1 is much larger than N_2 , the effects of N_2 can be neglected in the diluted PEO solutions [38, 39]. The elastic force F_E originates from an imbalance in the distribution of $N_1 = \tau_{xx} - \tau_{yy}$ over the size of the particle [40].

$$F_E \sim a^3 \nabla N_1 = a^3 (\nabla \tau_{xx} - \nabla \tau_{yy}) = 2a^3 (1 - \eta) W_i \nabla \hat{\gamma}^2 \quad (4)$$

where a is the particle diameter, η is the ratio of the solvent to solution viscosity and $\hat{\gamma}$ is the non-dimensional local shear rate.

2.3 Stokes drag

Drag force arises when an object moves in a different velocity with the corresponding fluid elements. The origin of the drag force lies in the need to displace the elements of the fluid out of the way of the moving object. The drag force on a moving spherical particle can be expressed by Stokes law:

$$\mathbf{F}_d = 3\pi\mu a (\mathbf{u}_f - \mathbf{u}_p) \quad (5)$$

where μ is dynamic viscosity of fluid, \mathbf{u}_f and \mathbf{u}_p are the velocity vectors of fluid and particles respectively.

2.4 Particle dynamics

Three forces act on particles suspended in a viscoelastic ferrofluid and the motion of particles is determined by the sum of these forces:

$$m_p \ddot{\mathbf{X}} = \mathbf{F}_m + \mathbf{F}_E + \mathbf{F}_d \quad (6)$$

where m_p and $\ddot{\mathbf{X}}$ are the mass and acceleration of particles. It should be noted that particles also experience other forces, such as gravity and buoyancy force, and they are negligible because the density of particles and the suspending medium are very close. In our design, the dominance of each force is implemented at different regions of the microchannel for the proper functionalities. In a straight channel with a square cross-section, the elastic force \mathbf{F}_E dominates the motion of particles, so that particles can be focused along the channel centreline. Then in the downstream, differential lateral migration of non-magnetic microparticles is controlled by the magnetophoretic force \mathbf{F}_m to enable size-based separation. At the end of the microchannel, separated particles follow the fluid streamline by the dominant Stokes drag \mathbf{F}_d and enter the corresponding outlets.

3. Materials and methods

3.1 Design and fabrication of microfluidic device

In this study, the microchannel in the microfluidic device consists of three straight channel sections, with dimensions of $50 \mu\text{m} \times 20 \text{ mm}$, $600 \mu\text{m} \times 10 \text{ mm}$, and $800 \mu\text{m} \times 5 \text{ mm}$ (width \times length), respectively. A linear expansion region between two sections was used to connect them smoothly. A rare earth neodymium (NdFeB) ($4 \text{ mm} \times 4 \text{ mm} \times 4 \text{ mm}$) was placed on one side of the second straight section with a lateral distance about 1 mm, Figure 1a. The height of the microchannel is uniformly $56 \mu\text{m}$, Figure 1b. Microfluidic devices were fabricated by the standard photolithography and soft lithography techniques [41]. A three-dimensional illustration of the microfluidic device and the image of a fabricated microfluidic device are shown in Figures 1c and 1d, respectively.

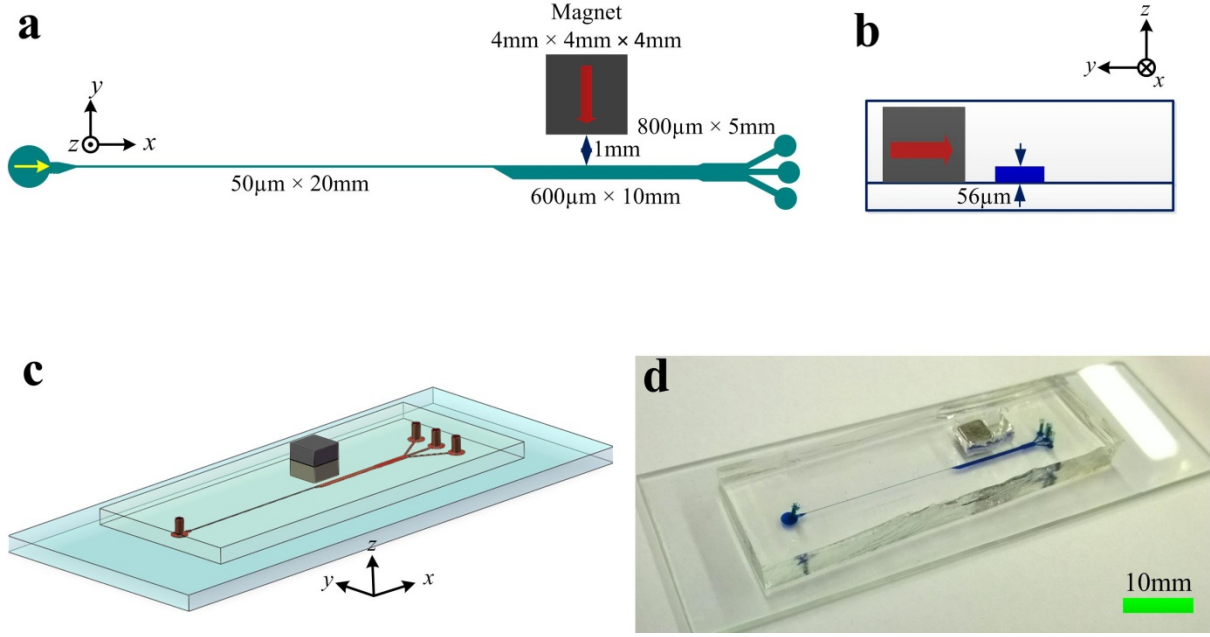


Figure 1 (a) The structure and dimensions of the microchannel used in the experiments. (b) Cross sectional view of the microchannel and magnet. (c) 3D illustration of the microfluidic device. (d) Image of the fabricated microfluidic device (the microchannel is filled with blue food dye for clarity).

3.2 Preparation of PEO-based ferrofluid and particle suspensions

PEO (poly (ethylene oxide), $M_w=2\,000\,000$, Sigma-Aldrich) aqueous solutions with concentrations of 1000ppm and 2000 ppm were first prepared by dissolving PEO powder in DI water. Then, mixing the PEO solution (2000 ppm) with a commercial water-based magnetite ferrofluid (EMG 408, Ferrotec Co., NH, volume ratio of the magnetite nanoparticles is 1.1%) and DI water in a ratio of 5:1:4 resulted in a ferrofluid with the PEO solution as the base medium. This novel fluid is called PEO-based ferrofluid. In this mixture, the PEO concentration is 1000 ppm, and the volume ratio of magnetite nanoparticles (mean diameter = 10.2nm) is 0.11%, which is 1/10 of the original ferrofluid. Meanwhile, the aqueous ferrofluid with the same volume ratio of magnetite nanoparticles of 0.11% was prepared by diluting the commercial ferrofluid with DI water by 10 times.

3.3 Particle preparation

Fluorescent polystyrene particles with a mean diameter of $a = 5\,\mu\text{m}$ (Product No. G0500, CV5%) and $13\,\mu\text{m}$ (Product No. 36-4, CV16%) were purchased from Thermo Fisher Scientific. In the verification tests, 5- μm particles were suspended in the proposed PEO-based ferrofluid, to confirm both features of viscoelastic focusing and negative

magnetophoresis in the proposed PEO-based ferrofluid. To conduct the separation tests, binary polystyrene beads mixture (5 μm and 13 μm) was suspended in the proposed PEO-based ferrofluid, as well as in the conventional aqueous ferrofluid for comparison. The concentrations of polystyrene particles in these suspensions are $\sim 10^6$ counts/ml. Tween 20 (Product No. P9416, Sigma-Aldrich,) with 0.1% w/v was added to prevent particles from aggregation.

3.4 Experimental setup

The NdFeB permanent magnet creates a non-uniform magnetic field. The magnet was placed on one side of wide microchannel as shown in Figure 1c. The magnetic flux density at the center of the magnet's pole surface was measured to be 120 mT by a Gauss meter (Model 5180, Pacific Scientific OECO). The magnetization direction of the magnet is perpendicular to the microchannel. The microfluidic device was placed on an inverted microscope (CKX41, Olympus), illuminated by a mercury arc lamp. Particle suspension was infused by a syringe pump (Legato 100, KD Scientific). The fluorescent images were captured by a high speed CCD camera (Optimos, Q-imaging, Australia), and then post-processed and analysed using the software Q-Capture Pro 7 (Q-imaging). The exposure time of each frame was 0.1 ms to capture images of single particle. To better observe the trajectories, 100 consecutive frames were merged together.

4. Results and Discussion

4.1 Negative magnetophoresis

To confirm the negative magnetophoresis in the PEO-based ferrofluid, 5- μm fluorescent polystyrene beads were dispersed in the proposed medium, and infused into a straight 600- μm wide microchannel. An NdFeB permanent magnet (cube, 4mm in length, height and width) was placed on one side of microchannel with a distance of 1 mm, and the flow rate was increased from 0.5 $\mu\text{l/min}$ to 15 $\mu\text{l/min}$ through a syringe pump. Figure 2 clearly shows that the non-magnetic particles are repelled from the permanent magnet and migrate toward the opposite side, which proves the existence of the negative magnetophoresis in the proposed PEO-based ferrofluid. In addition, we evaluated the negative magnetophoresis using a deflection angle θ , which is defined as the average ratio of lateral velocity to horizontal velocity of microparticles. Increasing flow rate from 0.5 $\mu\text{l/min}$ to 15 $\mu\text{l/min}$ decreases the deflection angle θ exponentially. And when the flow rate reaches 15 $\mu\text{l/min}$, it is hard to observe the obvious magnetophoretic deflection of particles in the designed microchannel. It should be noted that PEO-based ferrofluid has the property of viscoelasticity, then an elastic force F_E should exert on the micro-particles to push particles

along the gradient of fluid shear rate according to equation (4). However, due to the low aspect ratio (width/height) $\delta = 1/12$, the fluid velocity profile along a wide region of channel width is blunted with shear rate constantly zero (Supplementary Figure S1). So the elastic force which is proportional to the gradient of square of shear rate (equation (4)) is zero along a wide width region. Therefore, the influence of elastic force on the magnetophoresis is negligible in this situation.

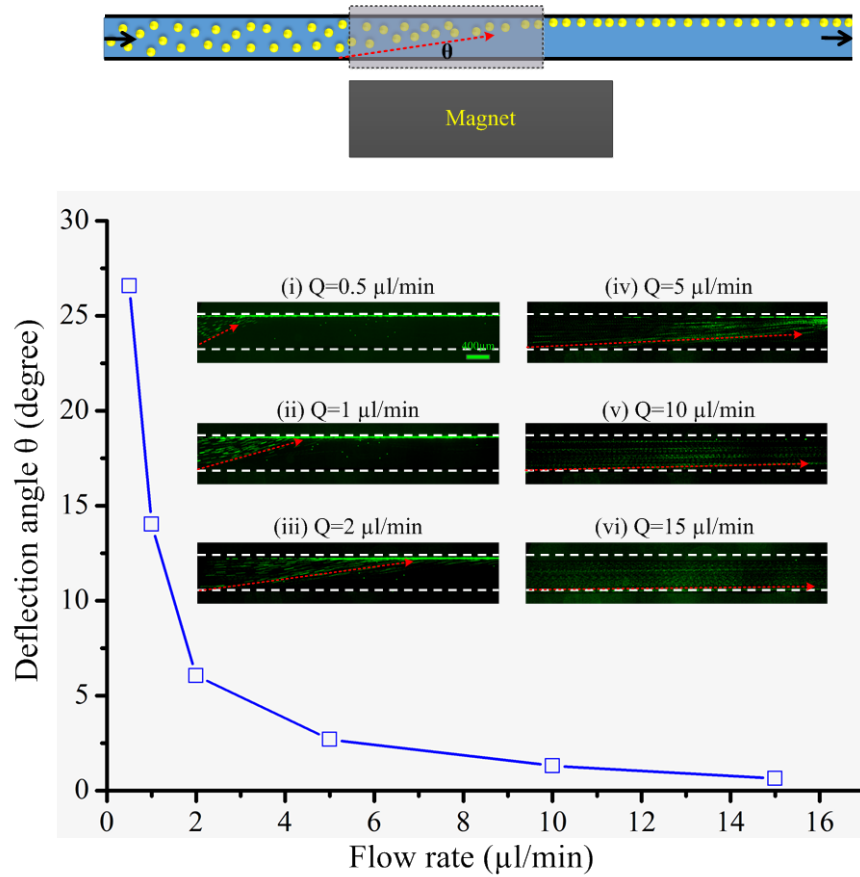


Figure 2 Negative magnetophoretic deflections of non-magnetic microparticles in the PEO-based ferrofluid under a non-uniform magnetic field. The deflection angle θ which is defined as the ratio of lateral velocity to horizontal velocity of microparticles decreases sharply with the increment of flow rate. Here, particle size is $5\mu\text{m}$, microchannel width is $600\mu\text{m}$, and lateral distance between microchannel and permanent magnet is 1 mm.

4.2 3D viscoelastic focusing

As we know, the viscoelasticity of polymer (PEO or PVP) or DNA solution with long chain molecules can focus micro-particles to the channel centerline or corners in a rectangular channel depending on the initial position of particles due to the gradient of the first normal stress difference [33, 36]. The number of multiple equilibrium positions can be reduced to

one at the centreline by increasing the flow rate due to the synergetic effects of inertia and viscoelasticity [37]. To confirm the viscoelastic focusing of microparticles in the proposed PEO-based ferrofluid, 5- μm fluorescent polystyrene beads suspended in the PEO-based ferrofluid were injected into a straight square-shaped microchannel at various flow rates from 5 $\mu\text{l/min}$ to 50 $\mu\text{l/min}$. As expected, the elastic effects due to the PEO molecule chains in the solution pinches the 5- μm particles gradually into the channel centreline along the channel length, and the existence of magnetite nanoparticles doesn't alter the viscoelastic focusing, Figure 3a. We also investigated the effects of flow rate on viscoelastic focusing in the PEO-based ferrofluid, Figure 3b. In good agreement with that of pure PEO solution, there is a flow rate threshold ($\sim 15 \mu\text{l/min}$) at which the particle focusing quality is optimal [37]. The particle focusing quality gets worse when the flow rate is below or above this threshold. The underlying mechanism of this phenomenon is the competition between the inertia and the elasticity. When the flow rate exceeds the threshold, the inertial lift forces which usually focus particles at the positions half-way between centreline and walls [12, 42] become much stronger than the elastic force, and deteriorate the centre-directed elastic focusing. However, if the flow rate is too small, inertial lift forces (specifically wall lift force) are too weak to repel particles near four corners towards the centreline, which is also not beneficial for particle focusing at the centreline.

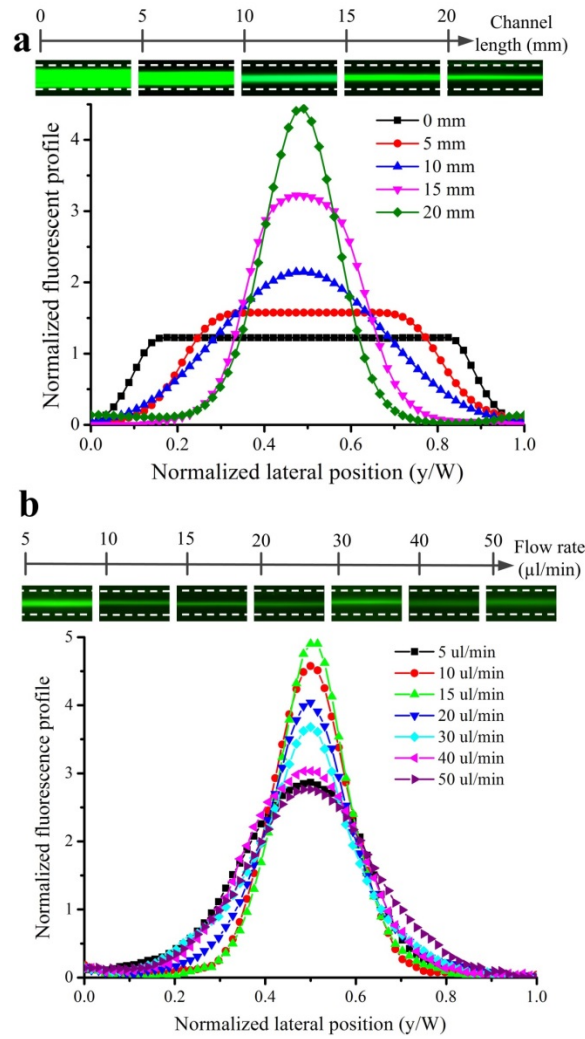


Figure 3 Viscoelastic 3D focusing of microparticles in a microchannel of $50\ \mu\text{m} \times 56\ \mu\text{m}$ (width \times height) (a) along channel length at a flow rate of $10\ \mu\text{l/min}$, and (b) under different flow rates after 20 mm distance. Particle diameter is $5\ \mu\text{m}$.

4.3 Sheathless separation of non-magnetic particles using the PEO-based ferrofluid

After confirming both properties for the proposed PEO-based ferrofluid, a microfluidic device was designed to employ both the features to efficiently separate non-magnetic particles. In order to simplify the design, the two properties of PEO-based ferrofluid were utilized individually in a serial manner. Figure 4a shows that after the introduction of binary micro-particles mixture, a straight microchannel with the square cross section is to focus all the microparticles to the channel centreline due to the elastic force (section I in Figure 4a); Then followed by an expand region, micro-particles enter a wide straight channel. A permanent magnet placed on one side of microchannel generates a non-uniform magnetic field and exerts a negative magnetophoretic force on the microparticles (section II in Figure 4a). Because the magnitude of magnetophoretic force is highly dependent on particle size,

larger particles experience much stronger magnetophoretic force and are repelled more quickly to the opposite wall than the smaller particles (as simulated in Figure 4b). Therefore, a size-dependent separation of non-magnetic particles in the PEO-based ferrofluid can be achieved (supplementary video S1). Here, the roles of a wide channel in section II include: (i) Slowing down the fluid speed from the upper stream, therefore the negative magnetophoretic force can overcome fluid drag force to repel particles toward the minima of the magnetic field; (ii) Low aspect ratio ($h/w \approx 1/12$) creates a blunted velocity profile along channel width as we discussed in the above ($u = 0$ and $\partial u / \partial y = 0$ for $0.1w < y < 0.9w$, Supplementary Figure S1), so that the effects of elastic force can be reduced to the minimum in section II. In the following, the 3D pre-focusing by elastic effects and size-dependent deflection will be demonstrated experimentally.

Figure 4 (a) Schematic illustration of microparticle viscoelastic 3D centreline focusing and magnetophoretic separation in the PEO-based ferrofluid. The viscoelastic effect of the novel ferrofluid is to focus randomly distributed microparticles at the inlet (A-A') into the channel centreline (B-B'). The expansion region is to decrease the linear fluid flow speed and particle movement speed, so that enough magnetophoretic force can exert on particles for enough time to deflect them. Large particles experience a stronger force and migrate to the opposite wall, while small particles move along the original path due to too the weak effects of magnetophoretic force. Therefore, a size-dependent separation of non-magnetic particles can be achieved (C-C'); (b) Numerical modeling of magnetophoretic separation of microparticles by size using COMSOL Multiphysics 5.1. Assuming the successful elastic focusing within the square channel, two differently-sized particles (5- μm and 13- μm) are released from the channel centreline section I, then both particles enter the wide channel (section II) where a non-uniform magnetic field is generated by a permanent magnet. Size-dependent magnetophoretic force exerts on the particles and enables particle separation.

In order to prove the validity of the design scheme, a particle mixture was prepared by suspending binary particles of 5- μm and 13- μm diameters in the PEO-based ferrofluid, and then infused into the microchannel at a flow rate of 15 $\mu\text{l/min}$. Figure 5 shows that the randomly distributed particles in the inlet (Figure 5a) migrate towards the channel centreline due to the effects of elastic force, and both 5- μm (green fluorescence) and 13- μm (red fluorescence) particles focus as a tight streak at the channel centreline after 20 mm (Figures 5b and 5c); After the expansion region, particles still remain as a compact streak even the

fluid streamline spreads during the expand region (Figure 5d); When the particles streak encounters the non-uniform magnetic field, larger particles (13- μm) undergo a negative magnetophoretic force 17 times stronger than that of their smaller counterparts (5- μm) because magnetophoretic force is proportional to the volume of particles according to equation (2). Therefore, 13- μm particles are deflected promptly to the opposite side, but the 5- μm particles almost maintain the original position with negligible deflection (Figure 5e). Finally, a bifurcation with three outlets embedded at the end of microchannel collects the corresponding sorted particles (Figure 5f, Supplementary video 2). However, if there is no magnet, both particle types will go straight without any deflection and enter the middle outlet (Figure S3). In addition, we also calculated the separation purity by examining particle mixture before and after separation in the hemocytometer (Figure 5g), and particle purities have been improved significantly from 45.8% to 90.8% for 13- μm particles and from 54.2% to 99.3% for 5- μm particles. This demonstrates the feasibility of the sheath-less separation of non-magnetic particles by employing the both properties of PEO-based ferrofluid in a single microfluidic device.

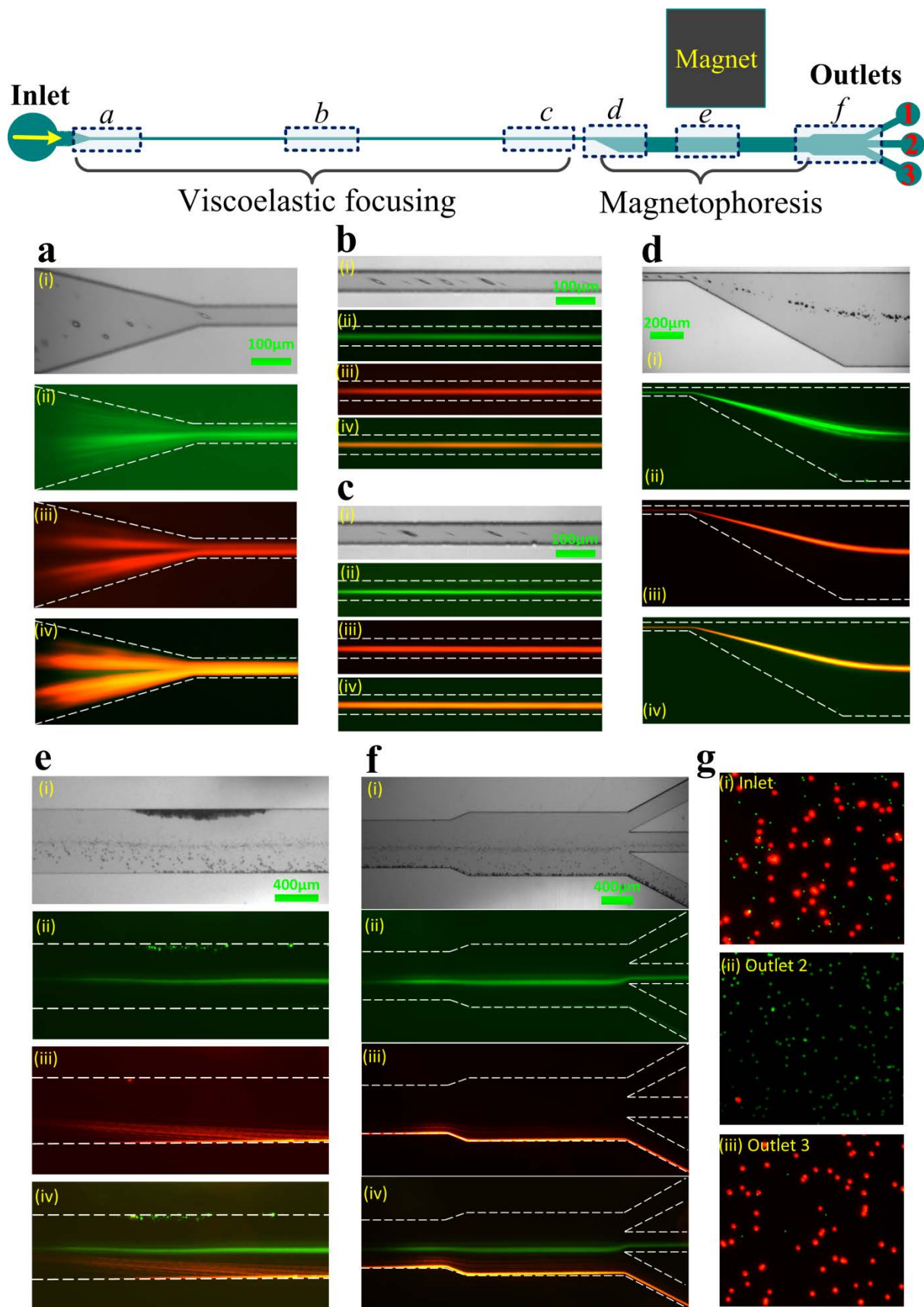


Figure 5 Sheath-less separation of non-magnetic particles using viscoelastic focusing and negative magnetophoresis using the PEO-based ferrofluid. (a)-(f) are particle trajectories in

Inlet, 10 mm downstream of the straight channel, 20 mm downstream of the straight channel, expansion area, magnet area, and outlet region, respectively. Within these images, (i) bright field images; (ii) and (iii) are fluorescent trajectories of 5- μm and 13- μm particles respectively; and (iv) Composed fluorescent images for the trajectories of 5- μm and 13- μm particles; (g) fluorescent images of the particle mixture in the hemocytometer before and after separation.

As a comparison, we also suspended 5- μm and 13- μm particles mixture in the conventional aqueous ferrofluid which has the same volume ratio of magnetite nanoparticles (0.11%), and tested their separation performance in the same microfluidic device at the flow rate of 15 $\mu\text{l}/\text{min}$. Particles randomly enter the inlet (Figure 6a), and still occupy a wide region of channel width even after 20 mm in the square channel because there is not any intrinsic or external force to focus particles (Figure 6b). When the wide particle streaks enter the magnetic region, 13- μm particles (red fluorescence) are repelled from the magnet due to the intense negative magnetophoretic force. However, the magnetophoretic force is too weak on 5- μm particles (green fluorescence) to deflect them, and they retain as a wide stripe (Figures 6c and 7a). At the outlet region, we can see that 5- μm particles exit from all the three outlets, hindering the efficient separation of particles (Figure 6d).

In contrast, for microparticles in the PEO-based ferrofluid, microparticles are confined to a tight lateral position before the magnetic region, and then the distance of binary particle streaks is big enough in the downstream for effective separation, Figure 7b. This further demonstrates the superior advantages of PEO-based ferrofluid in the manipulation of microparticles, and we believe that the proposed PEO-based ferrofluid will bring more flexibility and versatility in manipulation of microparticles. For example, in particle viscoelastic focusing, there are a few particles located at the four corners at relatively low flow rates. By patterning magnets symmetrically along two sides of microchannel, negative magnetophoretic forces will not only speed up the viscoelastic centreline focusing, but also may eliminate the particle focusing positions at four corners of cross section. In addition, negative magnetophoresis can be used to confine particles along one sidewall of channels, and in the downstream the elastic force with its magnitude proportional to the cubic of particle diameter (a^3) can enrich a size-dependent separation of microparticles. Furthermore, it would be very intriguing to couple magnetophoresis and elastic forces together to explore their complex interaction by delicately designing a microfluidic device to regulate their magnitude in the same order.

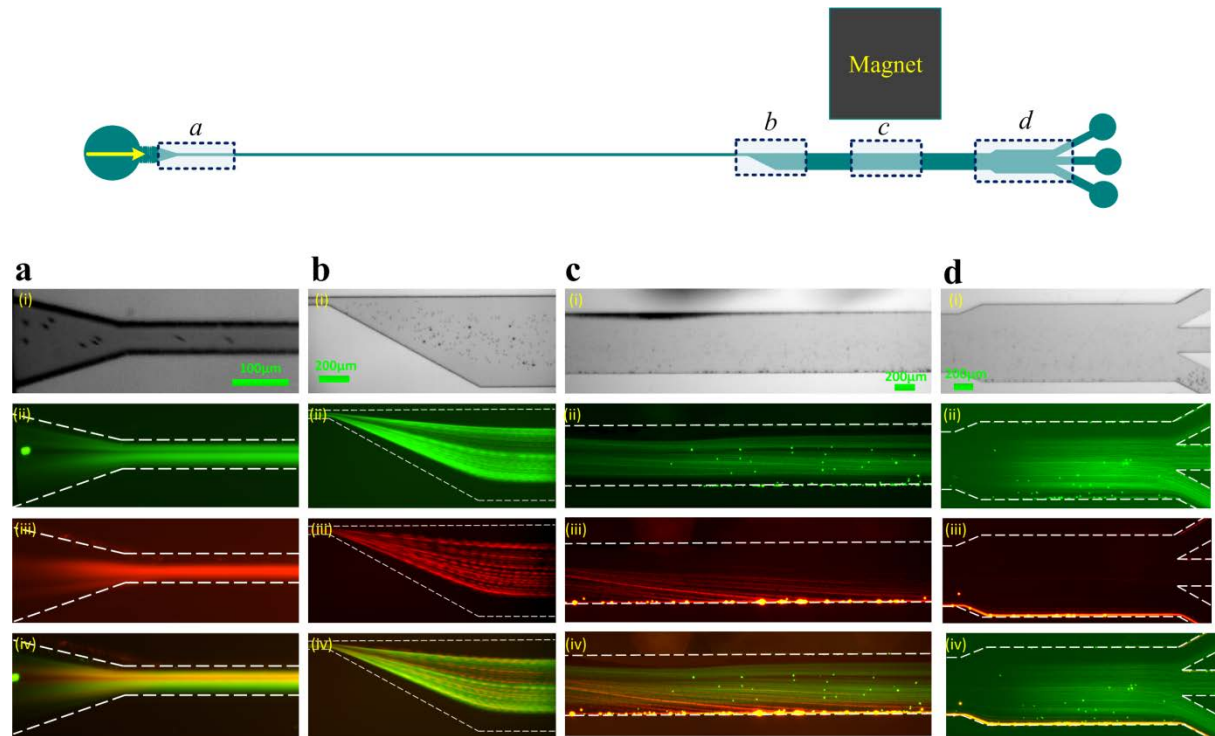


Figure 6 Particle magnetophoretic deflection in the microfluidic channel using the conventional aqueous ferrofluid. Particle trajectories at (a) inlet; (b) expand region; (c) magnet region; and (d) outlet region. Within these images, (i) bright field images; (ii) and (iii) fluorescent trajectories of 5- μm and 13- μm particles respectively; and (iv) merged fluorescent images of trajectories of 5- μm and 13- μm particles.

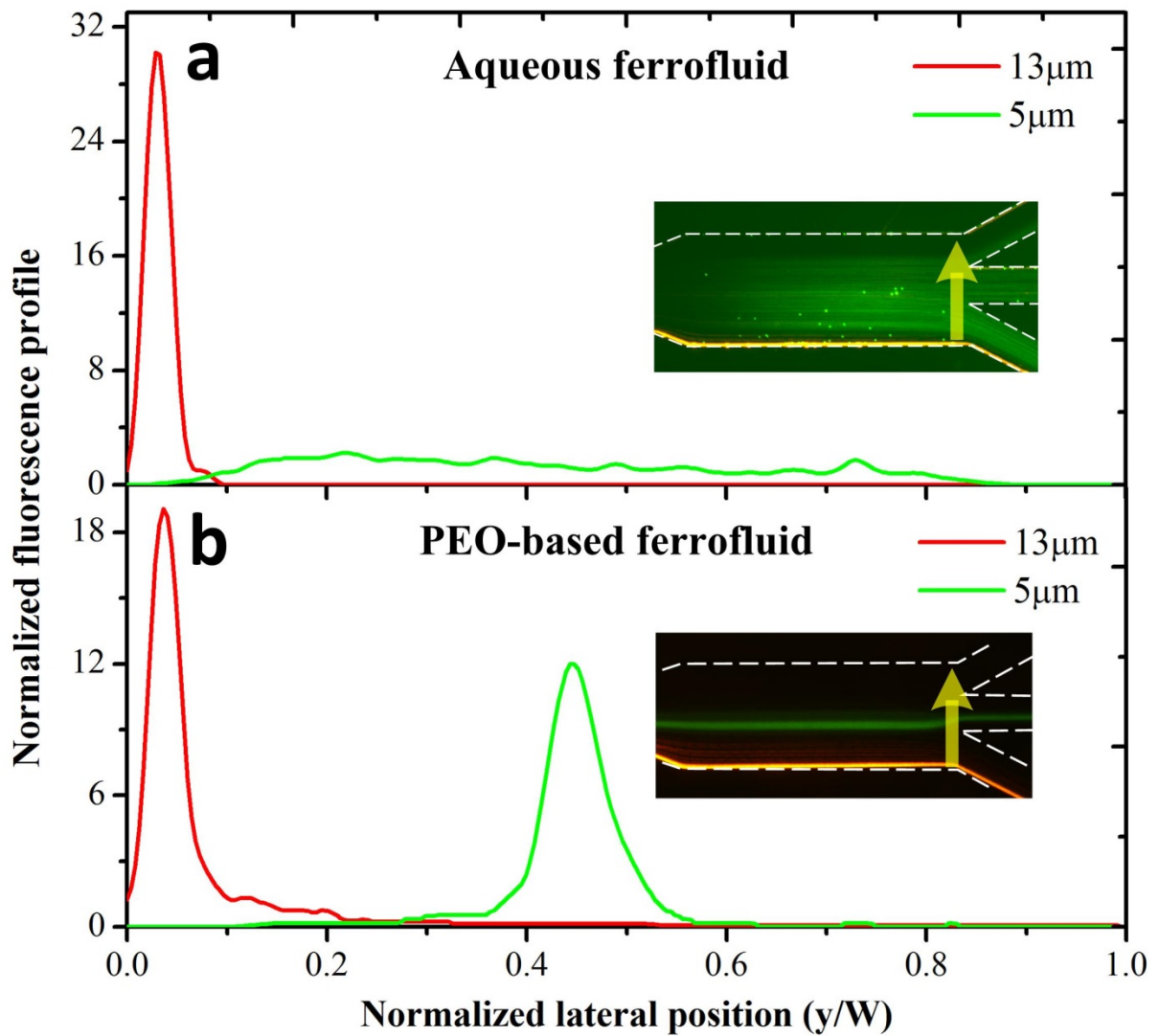


Figure 7 Normalized particles fluorescence profiles at the channel outlet for particles mixture in the conventional aqueous ferrofluid and the PEO-based ferrofluid.

Conclusions

In this work, we proposed and developed a novel viscoelastic ferrofluid by rendering the Newtonian base medium of the conventional ferrofluid with non-Newtonian viscoelastic PEO solution. And the properties of both viscoelastic centrelines focusing and negative magnetophoresis were demonstrated and investigated. By employing both viscoelastic and magnetic properties of the novel ferrofluid in a serial fashion, continuous and sheathless separation of non-magnetic microparticles based on particle size was achieved. As a comparison, we also tested the separation of non-magnetic particles in the conventional Newtonian ferrofluid, to further demonstrate the advantages of the viscoelastic-based ferrofluid. The novel viscoelastic-based ferrofluid is expected to bring more flexibility and versatility to the design and functionality in microfluidics.

Acknowledgements

This work is partially supported by the University of Wollongong-China Scholarship Council joint scholarships.

References

- [1] J. M. Martel, K. C. Smith, M. Dlamini, K. Pletcher, J. Yang, M. Karabacak, *et al.*, "Continuous Flow Microfluidic Bioparticle Concentrator," *Scientific reports*, vol. 5, p. Art No. 11300 2015.
- [2] J. Zhang, S. Yan, W. Li, G. Alici, and N.-T. Nguyen, "High throughput extraction of plasma using a secondary flow-aided inertial microfluidic device," *RSC Advances*, vol. 4, pp. 33149-33159, 2014.
- [3] J. Nam, B. Namgung, C. T. Lim, J.-E. Bae, H. L. Leo, K. S. Cho, *et al.*, "Microfluidic device for sheathless particle focusing and separation using a viscoelastic fluid," *Journal of Chromatography A*, vol. 1406, pp. 244-250, 2015.
- [4] P. R. Gascoyne and J. Vykoukal, "Particle separation by dielectrophoresis," *Electrophoresis*, vol. 23, p. 1973, 2002.
- [5] W. Zhao, T. Zhu, R. Cheng, Y. Liu, J. He, H. Qiu, *et al.*, "Label - Free and Continuous - Flow Ferrohydrodynamic Separation of HeLa Cells and Blood Cells in Biocompatible Ferrofluids," *Advanced Functional Materials*, vol. 26, pp. 3990 - 3998, 2015.
- [6] M. Hejazian, W. Li, and N.-T. Nguyen, "Lab on a chip for continuous-flow magnetic cell separation," *Lab on a Chip*, vol. 15, pp. 959-970, 2015.
- [7] P. Augustsson, C. Magnusson, M. Nordin, H. Lilja, and T. Laurell, "Microfluidic, Label-Free Enrichment of Prostate Cancer Cells in Blood Based on Acoustophoresis," *Analytical Chemistry*, vol. 84, pp. 7954-7962, 2012/09/18 2012.
- [8] M. MacDonald, G. Spalding, and K. Dholakia, "Microfluidic sorting in an optical lattice," *Nature*, vol. 426, pp. 421-424, 2003.
- [9] M. Pødenphant, N. Ashley, K. Koprowska, K. U. Mir, M. Zalkovskij, B. Bilenberg, *et al.*, "Separation of cancer cells from white blood cells by pinched flow fractionation," *Lab on a Chip*, vol. 15, pp. 4598-4606, 2015.
- [10] L. R. Huang, E. C. Cox, R. H. Austin, and J. C. Sturm, "Continuous particle separation through deterministic lateral displacement," *Science*, vol. 304, pp. 987-990, 2004.
- [11] S. Choi, S. Song, C. Choi, and J. K. Park, "Microfluidic self-sorting of mammalian cells to achieve cell cycle synchrony by hydrophoresis," *Analytical Chemistry*, vol. 81, pp. 1964-1968, 2009.
- [12] J. Zhang, S. Yan, D. Yuan, G. Alici, N.-T. Nguyen, M. Ebrahimi Warkiani, *et al.*, "Fundamentals and applications of inertial microfluidics: a review," *Lab on a Chip*, vol. 16, pp. 10-34, 2016.
- [13] A. Leshansky, A. Bransky, N. Korin, and U. Dinnar, "Tunable nonlinear viscoelastic "focusing" in a microfluidic device," *Physical review letters*, vol. 98, p. 234501, 2007.
- [14] M. Zborowski, J. J. Chalmers, and J. G. Webster, "Magnetophoresis: Fundamentals and Applications," in *Wiley Encyclopedia of Electrical and Electronics Engineering*, ed: John Wiley & Sons, Inc., 1999.
- [15] N. Pamme, "Magnetism and microfluidics," *Lab on a Chip*, vol. 6, pp. 24-38, 2006.

- [16] T. Zhu, R. Cheng, S. Lee, E. Rajaraman, M. Eiteman, T. Querec, *et al.*, "Continuous-flow ferrohydrodynamic sorting of particles and cells in microfluidic devices," *Microfluidics and Nanofluidics*, vol. 13, pp. 645-654, 2012/10/01 2012.
- [17] J. Zhu, L. Liang, and X. Xuan, "On-chip manipulation of nonmagnetic particles in paramagnetic solutions using embedded permanent magnets," *Microfluidics and nanofluidics*, vol. 12, pp. 65-73, 2012.
- [18] A. R. Kose, B. Fischer, L. Mao, and H. Koser, "Label-free cellular manipulation and sorting via biocompatible ferrofluids," *Proceedings of the National Academy of Sciences*, vol. 106, pp. 21478-21483, 2009.
- [19] A. I. Rodríguez-Villarreal, M. D. Tarn, L. A. Madden, J. B. Lutz, J. Greenman, J. Samitier, *et al.*, "Flow focussing of particles and cells based on their intrinsic properties using a simple diamagnetic repulsion setup," *Lab on a Chip*, vol. 11, pp. 1240-1248, 2011.
- [20] R. E. Rosensweig, "Magnetic fluids," *Annual review of fluid mechanics*, vol. 19, pp. 437-461, 1987.
- [21] L. Liang, J. Zhu, and X. Xuan, "Three-dimensional diamagnetic particle deflection in ferrofluid microchannel flows," *Biomicrofluidics*, vol. 5, p. 034110, 2011.
- [22] T. Zhu, F. Marrero, and L. Mao, "Continuous separation of non-magnetic particles inside ferrofluids," *Microfluidics and nanofluidics*, vol. 9, pp. 1003-1009, 2010.
- [23] L. Liang and X. Xuan, "Continuous sheath-free magnetic separation of particles in a U-shaped microchannel," *Biomicrofluidics*, vol. 6, p. 044106, 2012.
- [24] F. Shen, H. Hwang, Y. K. Hahn, and J.-K. Park, "Label-free cell separation using a tunable magnetophoretic repulsion force," *Analytical chemistry*, vol. 84, pp. 3075-3081, 2012.
- [25] J. Zeng, Y. Deng, P. Vedantam, T.-R. Tzeng, and X. Xuan, "Magnetic separation of particles and cells in ferrofluid flow through a straight microchannel using two offset magnets," *Journal of Magnetism and Magnetic Materials*, vol. 346, pp. 118-123, 2013.
- [26] G. D'Avino, G. Romeo, M. M. Villone, F. Greco, P. A. Netti, and P. L. Maffettone, "Single line particle focusing induced by viscoelasticity of the suspending liquid: theory, experiments and simulations to design a micropipe flow-focuser," *Lab on a Chip*, vol. 12, pp. 1638-1645, 2012.
- [27] F. Del Giudice, G. Romeo, G. D'Avino, F. Greco, P. A. Netti, and P. L. Maffettone, "Particle alignment in a viscoelastic liquid flowing in a square-shaped microchannel," *Lab on a Chip*, vol. 13, pp. 4263-4271, 2013.
- [28] X. Lu and X. Xuan, "Continuous microfluidic particle separation via elasto-inertial pinched flow fractionation," *Analytical chemistry*, vol. 87, pp. 6389-6396, 2015.
- [29] N. Xiang, X. Zhang, Q. Dai, J. Chen, K. Chen, and Z. Ni, "Fundamentals of elasto-inertial particle focusing in curved microfluidic channels," *Lab on a Chip*, vol. 16, pp. 2626-2635, 2016.
- [30] C. Liu, C. Xue, X. Chen, L. Shan, Y. Tian, and G. Hu, "Size-based separation of particles and cells utilizing viscoelastic effects in straight microchannels," *Analytical chemistry*, vol. 87, pp. 6041-6048, 2015.
- [31] D. Yuan, J. Zhang, S. Yan, G. Peng, Q. Zhao, G. Alici, *et al.*, "Investigation of particle lateral migration in sample - sheath flow of viscoelastic fluid and newtonian fluid," *Electrophoresis*, 2016.
- [32] K. W. Seo, Y. R. Ha, and S. J. Lee, "Vertical focusing and cell ordering in a microchannel via viscoelasticity: Applications for cell monitoring using a digital holographic microscopy," *Applied Physics Letters*, vol. 104, p. 213702, 2014.

- [33] K. Kang, S. S. Lee, K. Hyun, S. J. Lee, and J. M. Kim, "DNA-based highly tunable particle focuser," *Nature communications*, vol. 4, p. Art No. 2567, 2013.
- [34] F. Del Giudice, H. Madadi, M. M. Villone, G. D'Avino, A. M. Cusano, R. Vecchione, *et al.*, "Magnetophoresis 'meets' viscoelasticity: deterministic separation of magnetic particles in a modular microfluidic device," *Lab on a Chip*, vol. 15, pp. 1912-1922, 2015.
- [35] E. J. Lim, T. J. Ober, J. F. Edd, S. P. Desai, D. Neal, K. W. Bong, *et al.*, "Inertio-elastic focusing of bioparticles in microchannels at high throughput," *Nature communications*, vol. 5, p. Art No. 4120, 2014.
- [36] S. Cha, K. Kang, J. B. You, S. G. Im, Y. Kim, and J. M. Kim, "Hoop stress-assisted three-dimensional particle focusing under viscoelastic flow," *Rheologica Acta*, vol. 53, pp. 927-933, 2014.
- [37] S. Yang, J. Y. Kim, S. J. Lee, S. S. Lee, and J. M. Kim, "Sheathless elasto-inertial particle focusing and continuous separation in a straight rectangular microchannel," *Lab on a Chip*, vol. 11, pp. 266-273, 2011.
- [38] J. Magda, J. Lou, S. Baek, and K. DeVries, "Second normal stress difference of a Boger fluid," *Polymer*, vol. 32, pp. 2000-2009, 1991.
- [39] J. A. Pathak, D. Ross, and K. B. Migler, "Elastic flow instability, curved streamlines, and mixing in microfluidic flows," *Physics of Fluids (1994-present)*, vol. 16, pp. 4028-4034, 2004.
- [40] K. W. Seo, H. J. Byeon, H. K. Huh, and S. J. Lee, "Particle migration and single-line particle focusing in microscale pipe flow of viscoelastic fluids," *RSC Advances*, vol. 4, pp. 3512-3520, 2014.
- [41] D. C. Duffy, J. C. McDonald, O. J. A. Schueller, and G. M. Whitesides, "Rapid prototyping of microfluidic systems in poly (dimethylsiloxane)," *Analytical Chemistry*, vol. 70, pp. 4974-4984, 1998.
- [42] D. Di Carlo, "Inertial microfluidics," *Lab on a Chip*, vol. 9, pp. 3038-3046, 2009.